Supporting Information for the paper:

Sequential Dihydrogen Desorption from Hydride Protected Silver Clusters and the Formation of Naked Clusters in the Gas Phase

Atanu Ghosh, Mohammad Bodiuzzaman, Abhijit Nag, Madhuri Jash, Ananya Baksi and Thalappil Pradeep *

Department of Chemistry, DST Unit of Nanoscience (DST UNS) and Thematic Unit of Excellence (TUE), Indian Institute of Technology Madras, Chennai, 600 036, India

E-mail: pradeep@iitm.ac.in

Table of contents:

Experimental Section

Different instrumental conditions were used for the different type of measurements as shown below.

Synthesis of Ag_{17}^{+} ion from cluster I

Capillary voltage: 2kV

Sampling cone: 150 V (variable)

Source offset: 150 V

Source temperature: 100°C

Desolvation temperature: 150°C

Cone gas flow (L/Hr): 0

Desolvation gas flow (L/Hr): 400

Nebulizer gas flow (bar): 2.5

MS/MS of Ag_{17}^{+} ion

Capillary voltage: 2 kV

Sampling cone: 150 V

Source offset: 150 V

Source temperature: 100°C

Desolvation temperature: 150°C

Cone gas flow (L/Hr): 0

Desolvation gas flow (L/Hr): 400

Nebulizer gas flow (bar): 2.5

Trap collision energy: 200 (variable)

Synthesis of Ag_{19}^{+} from cluster III by MS/MS

Capillary voltage: 2.12 kV

Sampling cone: 0 V

Source offset: 0 V

Source temperature: 100°C

Desolvation temperature: 100°C

Cone gas flow (L/Hr): 0

Desolvation gas flow (L/Hr): 400

Nebulizer gas flow (bar): 2.5

Trap collision energy: 87 (variable)

Supporting Information 1

Characterizations of $[Ag_{22}(DPPE)_8H_{19}]^{3+}$ and $[Ag_{25}(DPPE)_8H_{22}]^{3+}$

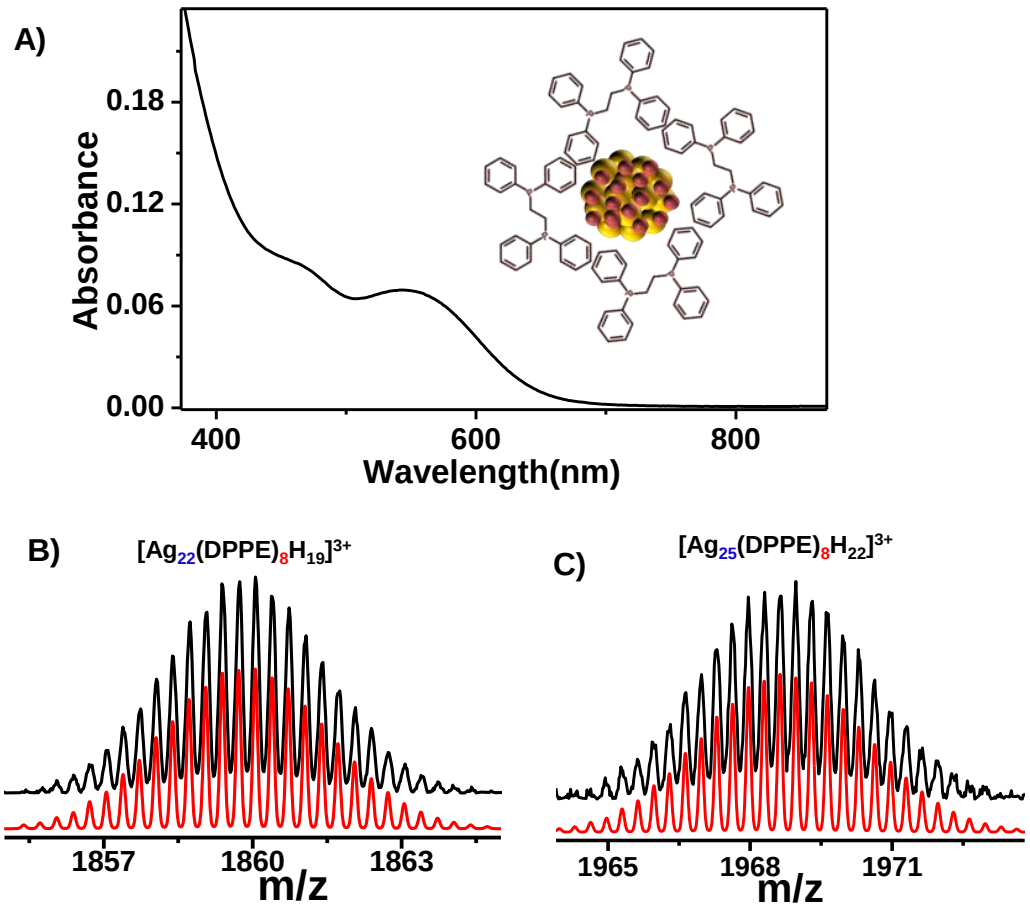

Figure S1. A) UV-vis spectrum of as synthesized mixture of clusters II and III. Inset: Schematic illustration of cluster. **B)** Comparison of experimental (black) and calculated (red) isotopic distribution of cluster III. **C)** Comparison of experimental (black) and calculated (red) isotopic distribution of cluster II. The UV-vis and mass spectra are match with the reported data.

Supporting Information 2

Naked cluster ions Ag_{21}^{+} and Ag_{19}^{+}

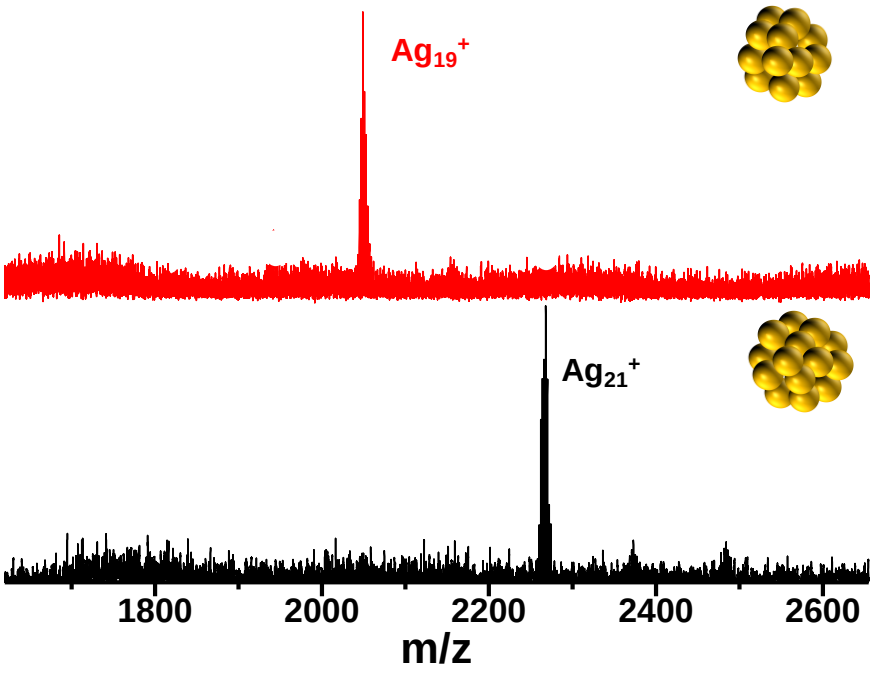

Figure S2. ESI MS spectra of naked cluster ions Ag_{19}^{+} (red trace) and Ag_{21}^{+} (black trace), synthesized from clusters II and III, respectively.

Supporting Information 3

Expanded region for Ag_6^+ and Ag_4^+ ions

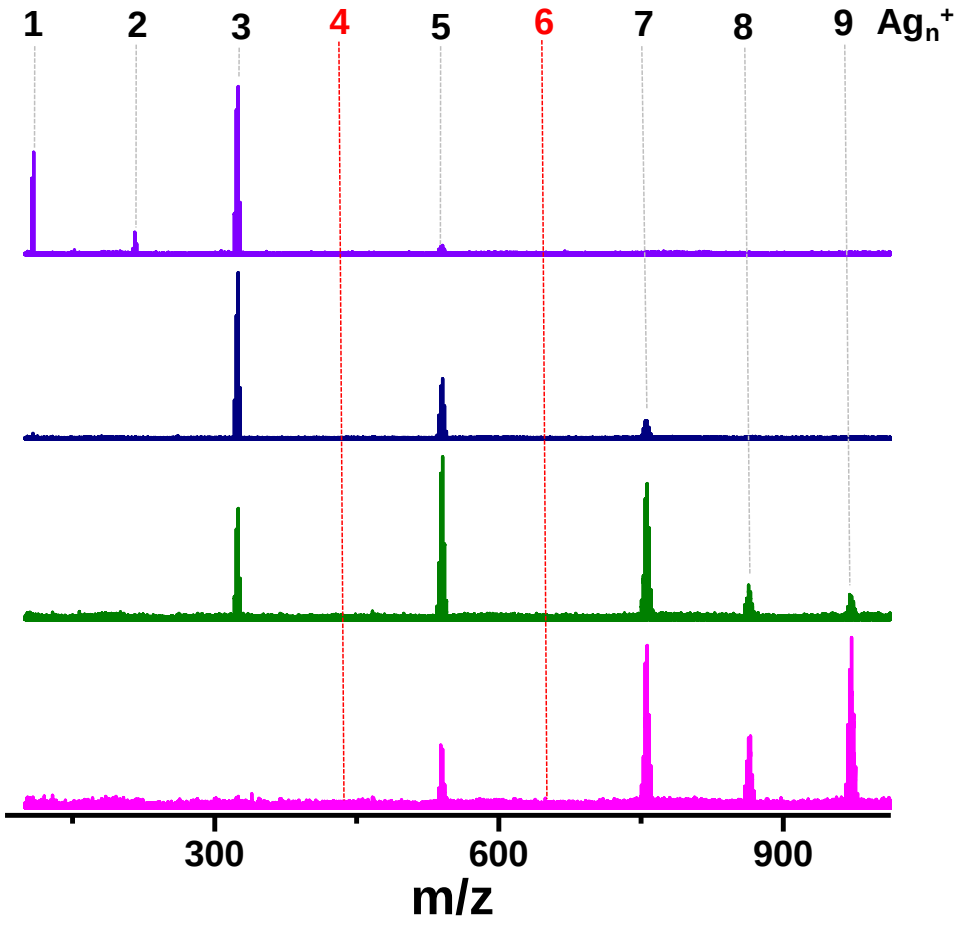

Figure S3. Ag_6^+ and Ag_4^+ regions from Figure 2 is expanded. All the ions from Ag_9^+ to Ag_1^+ are present except Ag_6^+ and Ag_4^+. Dotted red lines are used to mark the absence of Ag_6^+ and Ag_4^+ ions.

Supporting Information 4

Expanded region for Ag_{10}^{+} ion

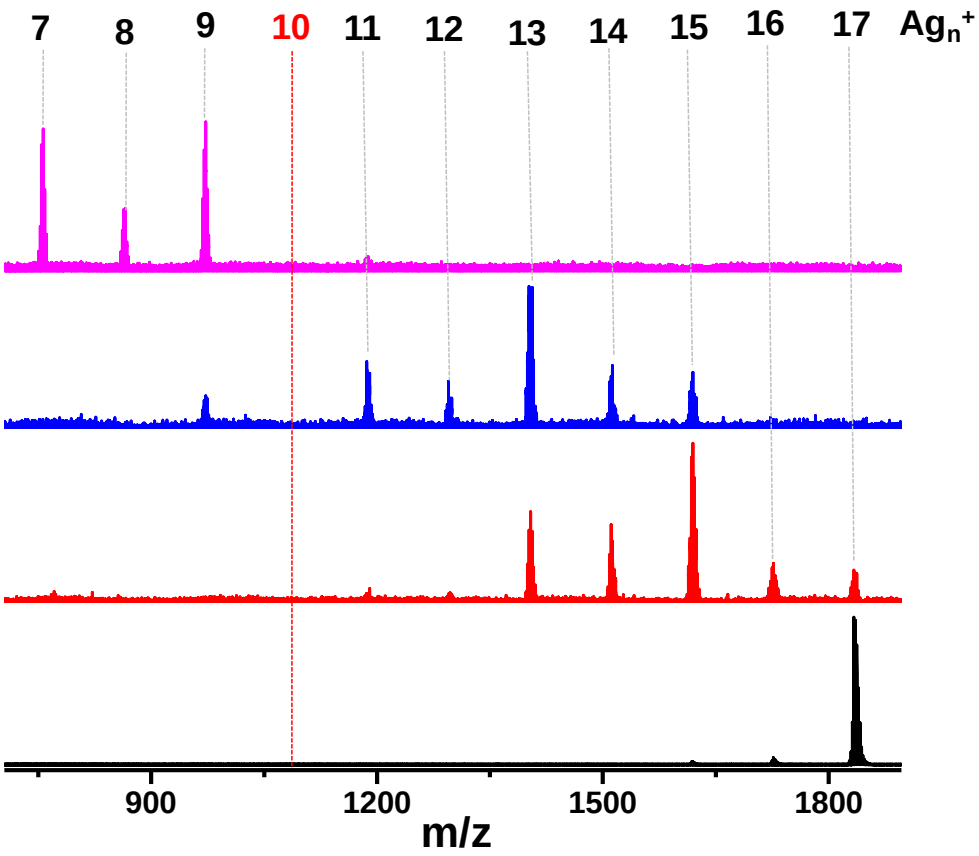

Figure S4. Ag_{10}^{+} region from Figure 2 is expanded. All the ions from Ag_{17}^{+} to Ag_{7}^{+} are present except Ag_{10}^{+}. Dotted red line is used to mark the absence of Ag_{10}^{+} ion.

Supporting Information 5

Isolation of $Ag_{17}H_{14}^{+}$ ion

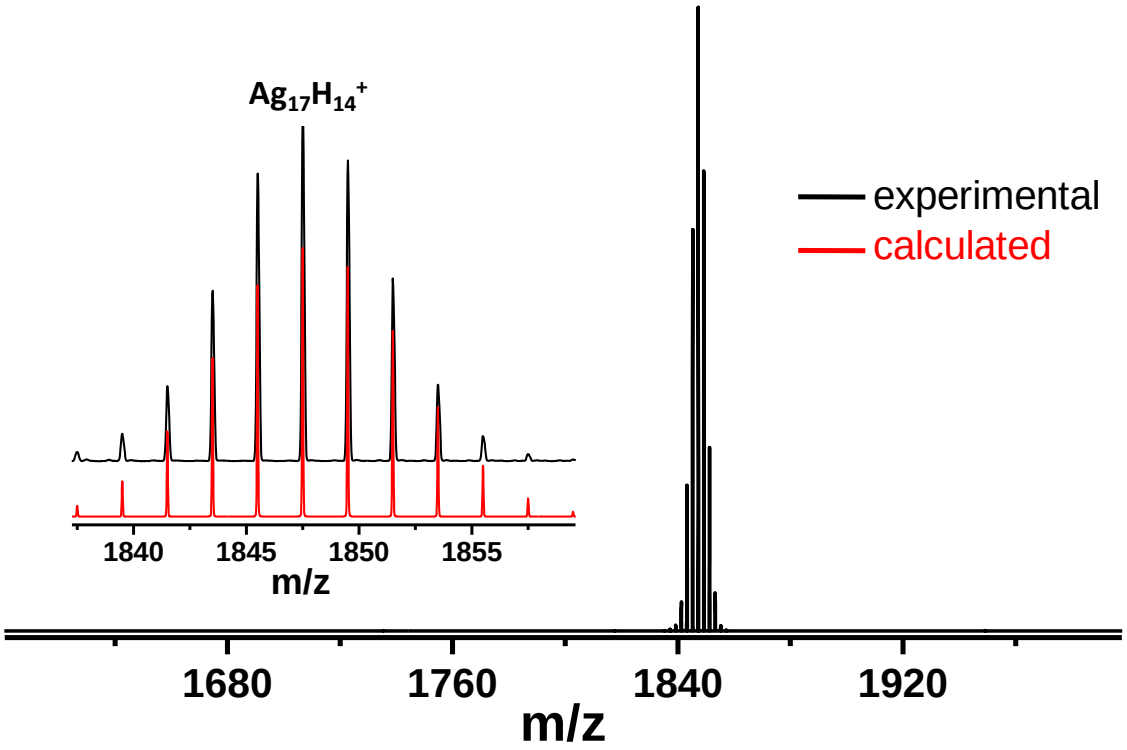

Figure S5. ESI MS spectrum of the ion which was formed during the formation of Ag_{17}^{+} ion from parent cluster I. Inset: Comparison of experimental (black) and calculated (red) spectra. The composition of the isolated ion is $Ag_{17}H_{14}^{+}$.

Supporting Information 6

ESI MS of $Ag_{17}H_{14}^{+}$ and $Ag_{17}D_{14}^{+}$

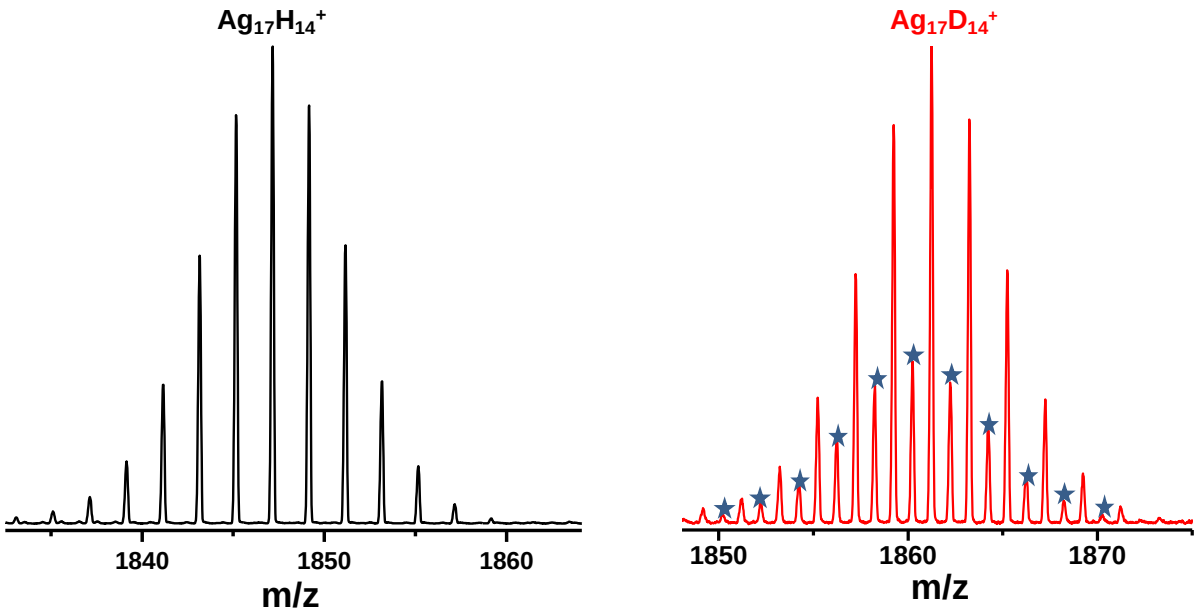

Figure S6. ESI MS spectra of $Ag_{17}H_{14}^{+}$ (m/z 1847, black trace) and $Ag_{17}D_{14}^{+}$ (m/z 1861, red trace) ions synthesized from $[Ag_{18}(TPP)_{10}H_{16}]^{2+}$ and $[Ag_{18}(TPP)_{10}D_{16}]^{2+}$, respectively. The peaks shown by asterisks (34% in intensity) in the spectrum of $Ag_{17}D_{14}^{+}$ are arising due to the presence of hydrogen, which are coming due to the partial isotope exchange (principally due to $Ag_{17}D_{13}H^{+}$) from non-deuterated solvents (methanol (MeOH) and water (H_2O)).

Supporting Information 7

Formation of Ag_{19}^{+} ion from cluster III

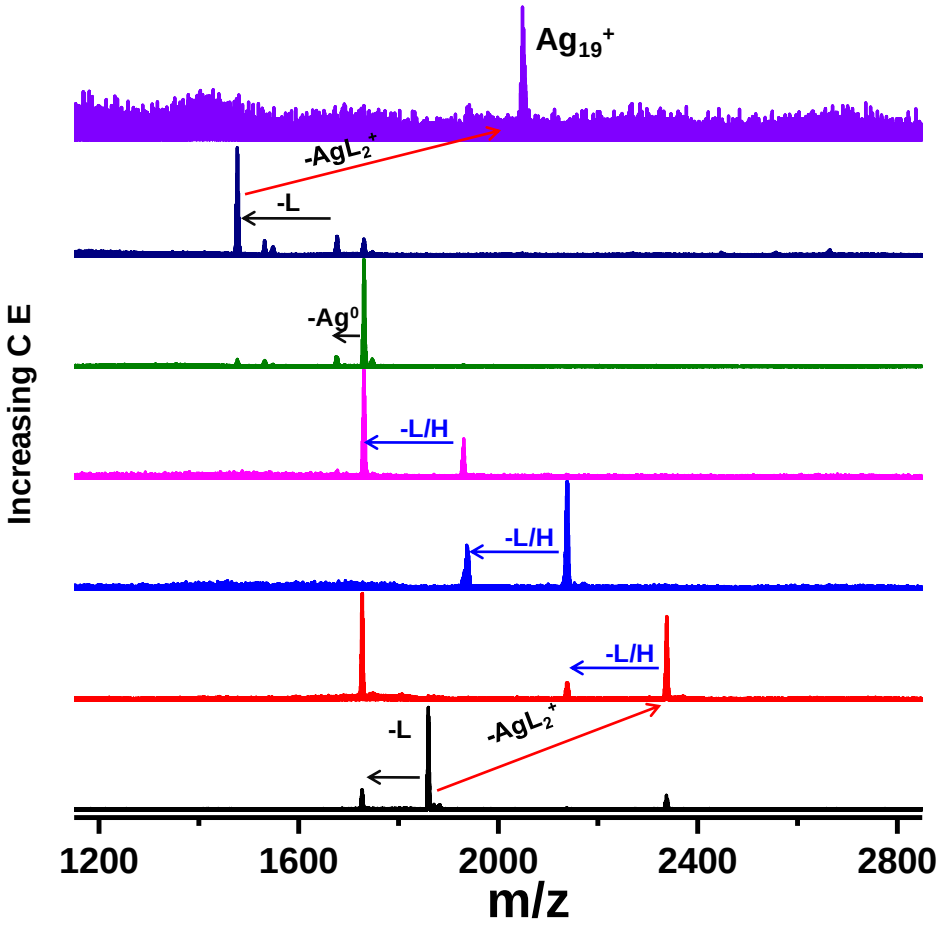

Figure S7. Collision energy-dependent fragmentation of cluster III. The process produces naked Ag_{19}^{+} cluster ion. L represents the DPPE ligand. Charge stripping and hydrogen loss steps are shown with red and blue arrows, respectively.

Supporting Information 8

Different ions formed during the formation of Ag_{19}^{+} ion

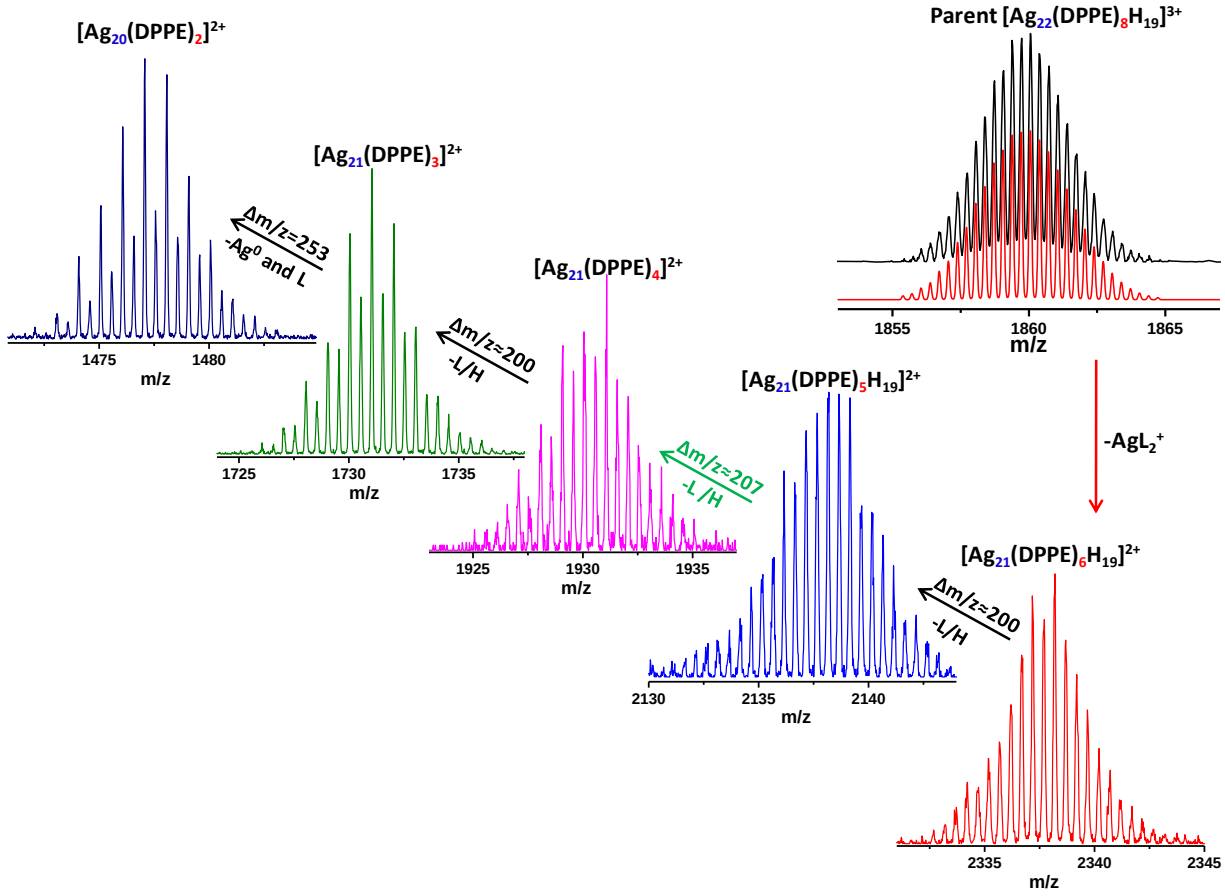

Figure S8. Peaks from Figure S7 are expanded here. Different ions formed during the formation of Ag_{19}^{+} ion. The charge stripping step is marked with the red arrow. Fragmentation step leading to the loss of maximum hydrogens is marked with the green arrow. Loss of sixteen hydrogens is observed at this step.

Supporting Information 9

Comparison with the deuterated analog of Cluster III

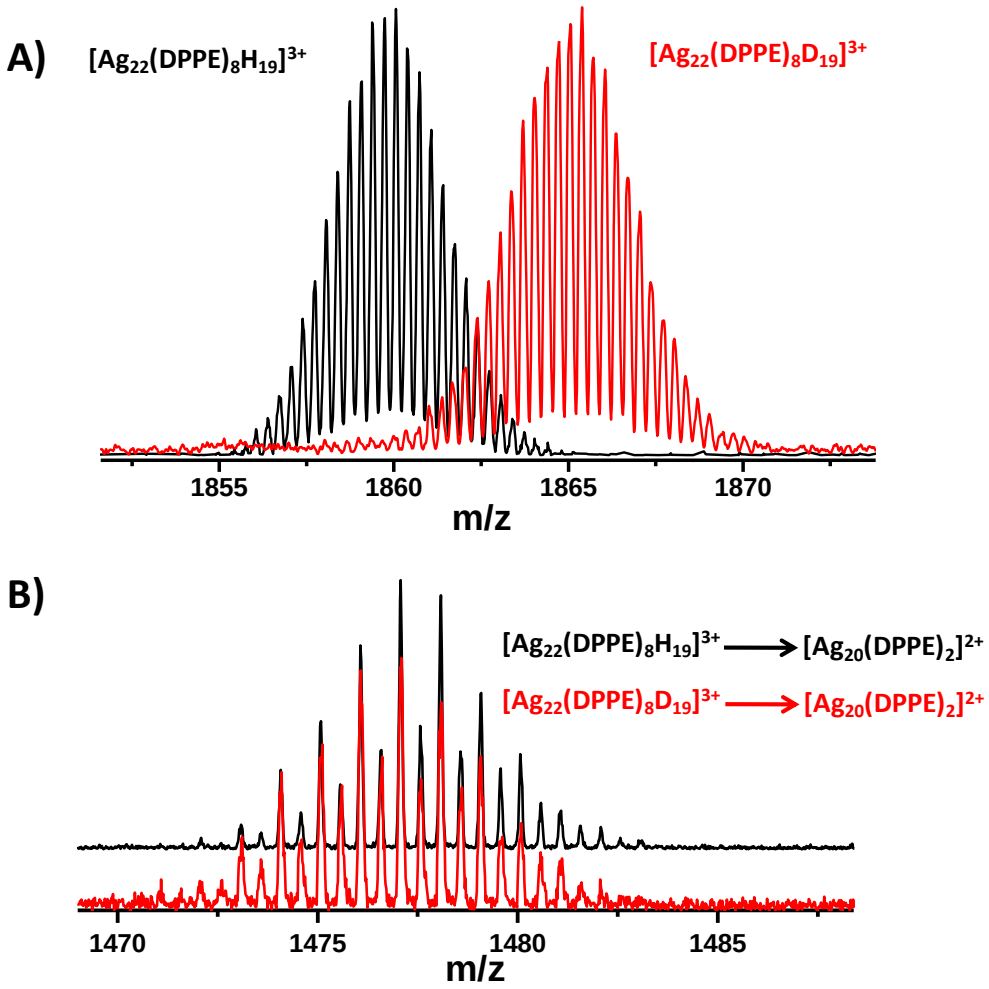

Figure S9. A) ESI MS spectra of the parent materials $[Ag_{22}(DPPE)_8H_{19}]^{3+}$ (black trace) and $[Ag_{22}(DPPE)_8D_{19}]^{3+}$ (red trace). **B)** $[Ag_{20}(DPPE)_2]^{2+}$cluster ions produced from the H (black trace) and D (red trace) protected parents clusters, respectively. Exact match of the isotopic distributions confirms the absence of hydrogen atoms in $[Ag_{20}(DPPE)_2]^{2+}$cluster ion.

Supporting Information 10

Comparison with the deuterated analog of Cluster II

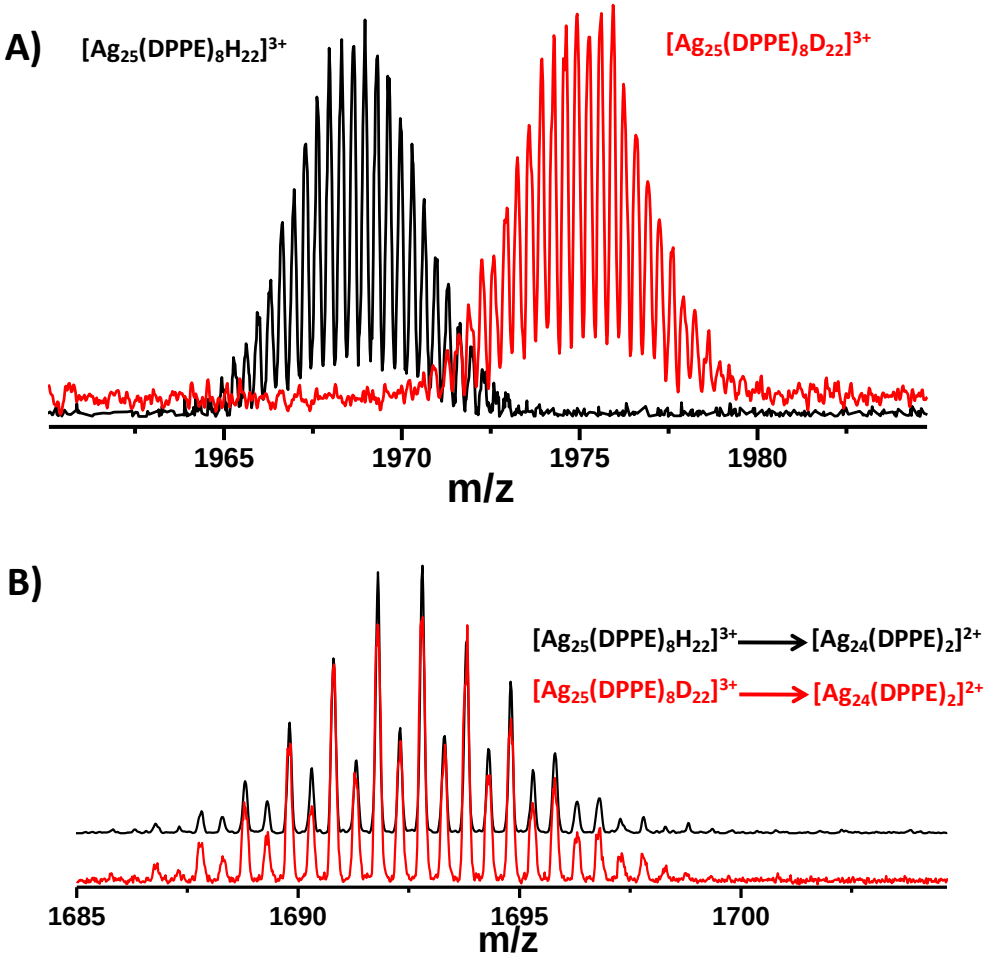

Figure S10. A) ESI MS spectra of the parent materials $[Ag_{25}(DPPE)_8H_{22}]^{3+}$ (black trace) and $[Ag_{25}(DPPE)_8D_{22}]^{3+}$ (red trace). **B)** $[Ag_{24}(DPPE)_2]^{2+}$cluster ions produced from H (black trace) and D (red trace) protected parents clusters, respectively. Exact match in the isotopic distributions confirms the absence of hydrogen atoms in $[Ag_{24}(DPPE)_2]^{2+}$cluster ion.

Supporting Information 11

Naked cluster ions Ag_{19}^{+} and Ag_{21}^{+}, synthesized from deuterated analogs of clusters II and III

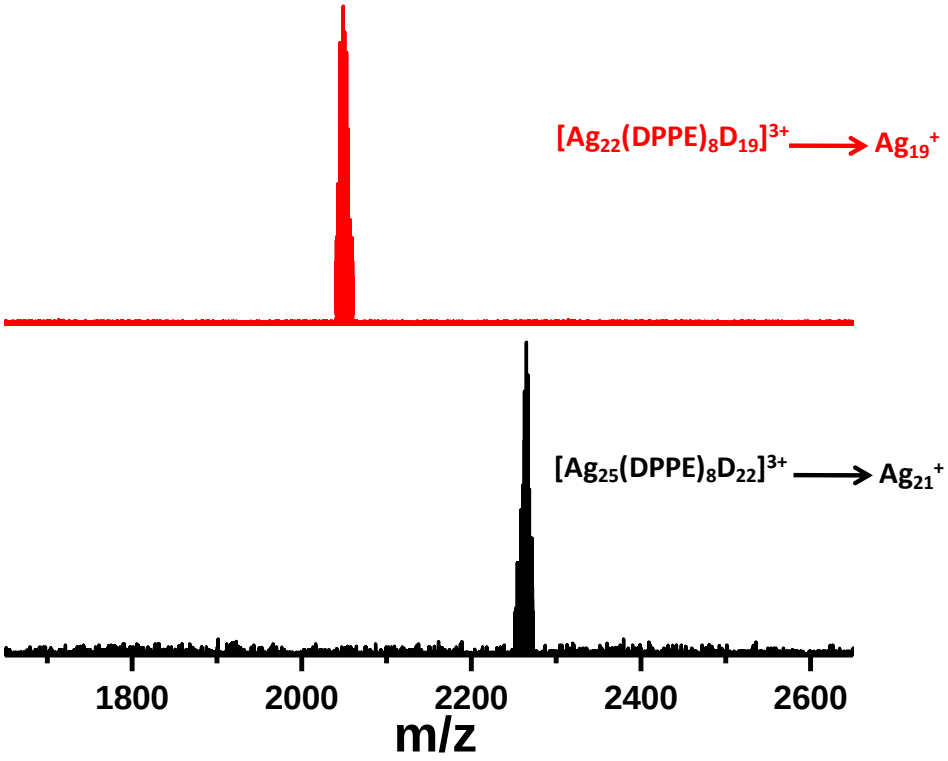

Figure S11. ESI MS spectra of naked cluster ions Ag_{19}^{+} (red trace) and Ag_{21}^{+} (black trace), synthesized from deuterated analogs of clusters II and III, respectively.

Supporting Information 12

Table S1: Comparison of positions of experimental and calculated spectra

Formula	**Calculated mass (m/z)**	**Experimental mass (m/z)**
$[Ag_{18}TPP_{10}H_{16}]^{2+}$	2290.1	2290.0
$[Ag_{18}TPP_{9}H_{16}]^{2+}$	2159.0	2158.9
$[Ag_{18}TPP_{8}H_{16}]^{2+}$	2028.1	2028.0
$[Ag_{18}TPP_{7}H_{16}]^{2+}$	1897.1	1897.1
$[Ag_{18}TPP_{6}H_{16}]^{2+}$	1765.5	1765.4
$[Ag_{18}TPP_{5}H_{16}]^{2+}$	1634.4	1634.3
$[Ag_{17}TPP_{3}H_{16}]^{+}$	2635.6	2635.5
$[Ag_{17}TPP_{2}H_{16}]^{+}$	2373.5	2373.4
$[Ag_{17}H_{14}]^{+}$	1847.2	1847.2
Ag_{17}^{+}	1833.1	1833.1